Transient response of isotropic, orthotropic and anisotropic composite-sandwich shells with the superparametric element

Mallikarjuna [a], T. Kant [b] and M. Fafard [a]

[a] *Civil Engineering Department, Laval University, Québec, Canada G1K 7P4*
[b] *Civil Engineering Department, Indian Institute of Technology, Bombay 400 076, India*

Abstract. The first-order Reissner–Mindlin shear deformation theory (FOST) is employed to investigate the transient response of isotropic, layered orthotropic and anisotropic composite and sandwich shells. The eight-noded Serendipity and nine-noded Lagrangian quadrilateral superparametric shell elements are used. Numerical convergence and stability of the elements are established using an explicit central difference technique with a special mass matrix diagonalization scheme. The effects of transverse shear moduli of stiff layers, length/thickness and radius/length ratios, time step, finite element mesh, orientation of fibers and degree of orthotropy on the transient response of shells are studied. The variety of results presented here, based on realistic material properties of more commonly used advanced laminated composite shells, should serve as references for future investigations.

Introduction

The increased use of fiber-reinforced composites for high-performance design applications necessitates more realistic prediction of the response characteristics of composite and sandwich shells. Most structures, whether they are used in land, sea or air, are subjected to dynamic loads during their operation. Therefore, there exists a need for assessing the transient analysis of laminated shells. To date, however, transient response of composite-sandwich shells of finite dimensions have not received adequate consideration.

A large amount of literature has been devoted to the development of theories for conventional sandwich structures and to the study of their static and dynamic behaviors by analytical and numerical methods. A detailed historical review is given in two books by Plantema [1] and Allen [2] and in two papers by Habip [3,4]. The pioneer worker was Reissner [5,6], who also studied the finite deflection problem. A few researchers [7,8] have adopted the finite element method in analyzing conventional sandwich shells. In the present paper, the transient response of layered, composite-sandwich shells is investigated using a shear deformable finite element. The Hughes–Liu element [9] is a degenerated 3-D element, an approach originally presented by Ahmad et al. [10] and used by many others [11–13]. The present 2-D finite element formulation is based on Ahmad's shell element [10] and is extended for the analysis of fiber-reinforced laminated orthotropic/anisotropic shell structures. This study is the continuation of the present authors' earlier work [14] on anisotropic sandwich plates.

Correspondence to: Dr. Mallikarjuna, Civil Engineering Department, Laval University, Québec, Canada G1K 7P4.

Apparently, the present study is the first to consider the transient dynamic analysis of fiber-reinforced laminated anisotropic sandwich shell structures using a superparametric element.

Equations of motion

Finite element spatial discretization schemes, when applied to structural dynamic analysis problems, result in a set of ordinary differential equations. In the absence of damping, these equations take the form

$$M\ddot{a}(t) + Ka(t) = q(t), \tag{1}$$

in which the dots define differentiation with time, $a(t)$ is the nodal displacement vector, M and K are the mass and stiffness matrices respectively, and $q(t)$ is the vector of external forces which varies with time t.

Element stiffness and mass

A typical quadrilateral shell element and the three types of coordinates, viz. nodal, local and global, are shown in Fig. 1. The geometric definition of the element is given in Ref. [13].
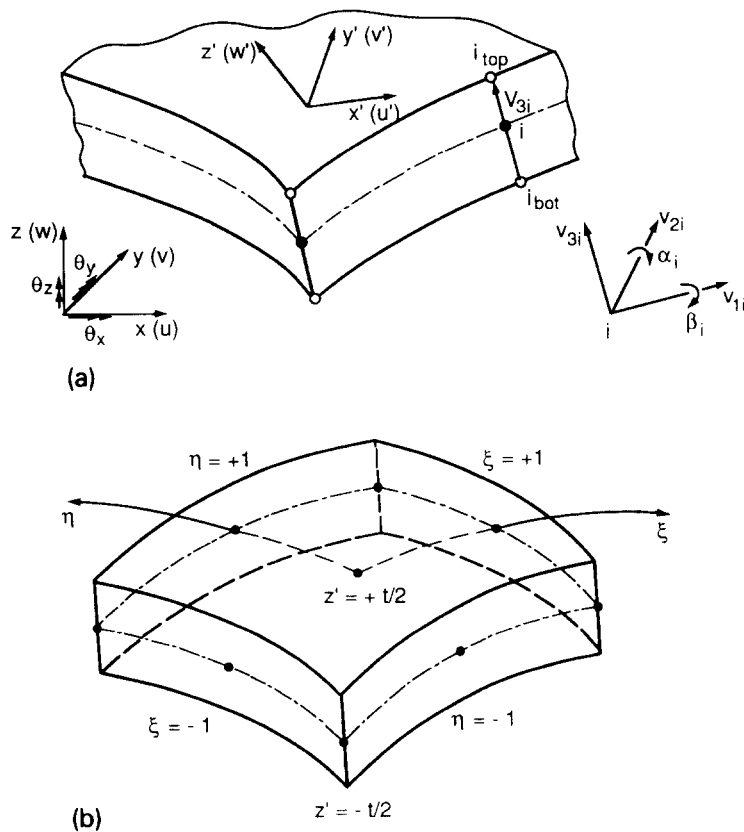

Fig. 1. (a) Local and global coordinates. (b) A typical none-noded shell element.

The displacement components u_i, v_i and w_i are the midsurface nodal displacements in the x, y and z global coordinate directions, α_i and β_i are the rotations about the v_{2i} and v_{1i} axes respectively. The vectors $\vec{v}_{1i}$, $\vec{v}_{2i}$ and $\vec{v}_{3i}$ are mutually perpendicular. It is therefore conceivable that in the assembled structure, no two nodal rotation vectors will have the same direction. Vector $\vec{v}_{3i}$ is defined by input data, and is presumed to span the thickness and to be normal to the midsurface. The displacements at any point (ξ, η, z') can be expressed in terms of the nodal displacements as,

$$\begin{Bmatrix} u \\ v \\ w \end{Bmatrix} = \sum_{i=1}^{NN} N_i(\xi, \eta) \begin{Bmatrix} u_i \\ v_i \\ w_i \end{Bmatrix} + \sum_{i=1}^{NN} N_i(\xi, \eta) z' \begin{bmatrix} l_{1i} & -l_{2i} \\ m_{1i} & -m_{2i} \\ n_{1i} & -n_{2i} \end{bmatrix} \begin{Bmatrix} \alpha_i \\ \beta_i \end{Bmatrix}. \tag{2}$$

The normal rotations α_i and β_i can be expressed in terms of global rotations θ_{xi}, θ_{yi} and θ_{zi} at each node i about the global axes x, y and z directions, respectively as

$$\theta_{xi} = l_{2i}\alpha_i + l_{1i}\beta_i, \qquad \theta_{yi} = m_{2i}\alpha_i + m_{1i}\beta_i, \qquad \theta_{zi} = n_{2i}\alpha_i + n_{1i}\beta_i. \tag{3}$$

The shape functions used for describing the geometry of the element and displacement variation are expressed in the natural coordinates (ξ, η). The relationship between the natural and local coordinate systems can be computed by using the chain rule of partial differentiation and is given in Ref. [13].

The local system of axes is the most convenient system for expressing the stress components and their resultants for shell analysis and design. If at any point on the mid-surface, a normal z' is erected with two other orthogonal axes x' and y' tangent to it (Fig. 1), the strain components of interest are given simply by the three-dimensional relationships. To more easily deal with the shell assumption of zero normal stress in the z'-direction ($\sigma_{z'} = 0$), the strain components should be defined in terms of the local system of axes x', y', z'. The linear midplane strain–displacement relationship can now be written as follows:

$$\epsilon_{x'_0} = \left(\frac{\partial u'}{\partial x'} \right)_0 = \sum_{i=1}^{NN} \frac{\partial N_i}{\partial x'} \left(\bar{l}_1 u_i + \bar{m}_1 v_i + \bar{n}_1 w_i \right),$$

$$\epsilon_{y'_0} = \left(\frac{\partial v'}{\partial y'} \right)_0 = \sum_{i=1}^{NN} \frac{\partial N_i}{\partial y'} \left(\bar{l}_2 u_i + \bar{m}_2 v_i + \bar{n}_2 w_i \right),$$

$$\gamma_{x'y'_0} = \left(\frac{\partial u'}{\partial y'} \right)_0 + \left(\frac{\partial v'}{\partial x'} \right)_0 = \sum_{i=1}^{NN} \frac{\partial N_i}{\partial y'} \left(\bar{l}_1 u_i + \bar{m}_1 v_i + \bar{n}_1 w_i \right) + \frac{\partial N_i}{\partial x'} \left(\bar{l}_2 u_i + \bar{m}_2 v_i + \bar{n}_2 w_i \right),$$

$$\chi_{x'} = \frac{\partial \theta_{y'}}{\partial x'} = \sum_{i=1}^{NN} \frac{\partial N_i}{\partial x'} \left[\alpha_i \left(\bar{l}_2 l_{2i} + \bar{m}_2 m_{2i} + \bar{n}_2 n_{2i} \right) \right.$$
$$\left. + \beta_i \left(\bar{l}_2 l_{1i} + \bar{m}_2 m_{1i} + \bar{n}_2 n_{1i} \right) \right],$$

$$\chi_{y'} = \frac{-\partial \theta_{x'}}{\partial y'} = -\sum_{i=1}^{NN} \frac{\partial N_i}{\partial y'} \left[\alpha_i \left(\bar{l}_1 l_{2i} + \bar{m}_1 m_{2i} + \bar{n}_1 n_{2i} \right) \right.$$
$$\left. + \beta_i \left(\bar{l}_1 l_{1i} + \bar{m}_1 m_{1i} + \bar{n}_1 n_{1i} \right) \right], \tag{4}$$

$$\chi_{x'y'} = \frac{\partial \theta_{y'}}{\partial y'} - \frac{\partial \theta_{x'}}{\partial x'}$$

$$= \sum_{i=1}^{NN} \frac{\partial N_i}{\partial y'} \left[\alpha_i \left(\bar{l}_2 l_{2i} + \bar{m}_2 m_{2i} + \bar{n}_2 n_{2i} \right) + \beta_i \left(\bar{l}_2 l_{1i} + \bar{m}_2 m_{1i} + \bar{n}_2 n_{1i} \right) \right]$$

$$- \frac{\partial N_i}{\partial x'} \left[\alpha_i \left(\bar{l}_1 l_{2i} + \bar{m}_1 m_{2i} + \bar{n}_1 n_{2i} \right) + \beta_i \left(\bar{l}_1 l_{1i} + \bar{m}_1 m_{1i} + \bar{n}_1 n_{1i} \right) \right],$$

$$\gamma_{y'z'} = \frac{\partial w'}{\partial y'} - \theta_{x'} = \sum_{i=1}^{NN} \frac{\partial N_i}{\partial y'} \left(\bar{l}_3 u_i + \bar{m}_3 v_i + \bar{n}_3 w_i \right)$$

$$- N_i \left[\alpha_i \left(\bar{l}_1 l_{2i} + \bar{m}_1 m_{2i} + \bar{n}_1 n_{2i} \right) + \beta_i \left(\bar{l}_1 l_{1i} + \bar{m}_1 m_{1i} + \bar{n}_1 n_{1i} \right) \right],$$

$$\gamma_{x'z'} = \frac{\partial w'}{\partial x'} + \theta_{y'} = \sum_{i=1}^{NN} \frac{\partial N_i}{\partial x'} \left(\bar{l}_3 u_i + \bar{m}_3 v_i + \bar{n}_3 w_i \right)$$

$$+ N_i \left[\alpha_i \left(\bar{l}_2 l_{2i} + \bar{m}_2 m_{2i} + \bar{n}_2 n_{2i} \right) + \beta_i \left(\bar{l}_2 l_{1i} + \bar{m}_2 m_{1i} + \bar{n}_2 n_{1i} \right) \right].$$

where l, m and n represent the direction cosines, and NN is the number of nodes per element.

The generalized strain tensor $\bar{\epsilon}'$ at any point in the local coordinate system can be expressed by the following relation:

$$\bar{\epsilon}' = \sum_{i=1}^{NN} B_i \delta_i, \tag{5a}$$

where

$$\bar{\epsilon}' = \left[\epsilon_{x_0'}, \ \epsilon_{y_0'}, \ \gamma_{x'y_0'}, \ \chi_{x'}, \ \chi_{y'}, \ \chi_{x'y'}, \ \gamma_{x'z_0'}, \ \gamma_{y'z_0'} \right]^{\mathrm{T}}, \tag{5b}$$

$$\delta_i = \left[u_i, \ v_i, \ w_i, \ \alpha_i, \ \beta_i \right]^{\mathrm{T}}. \tag{5c}$$

and B is the strain–displacement matrix defined in terms of the displacement derivatives with respect to the local Cartesian coordinates x', y', z' by eqn. (4). The components of the membrane force, bending moment and shear force vectors are defined as,

$$\begin{bmatrix} N_{x'} & N_{y'} & N_{x'y'} \\ M_{x'} & M_{y'} & M_{x'y'} \end{bmatrix} = \sum_{L=1}^{NL} \int_{h_l}^{h_{L+1}} \left[\sigma_{x'}, \ \sigma_{y'}, \ \tau_{x'y'} \right] \begin{bmatrix} 1 \\ z' \end{bmatrix} \mathrm{d}z', \tag{6a}$$

$$\left[Q_{x'} \quad Q_{y'} \right] = \sum_{L=1}^{NL} \int_{h_l}^{h_{L+1}} \left[\tau_{x'z'} \quad \tau_{y'z'} \right] \mathrm{d}z. \tag{6b}$$

Upon integration, these expressions are rewritten in a concise matrix form which defines the stress-resultant/strain relations of the layered sandwich shell and which is given by

$$\bar{\sigma}' = D \bar{\epsilon}', \tag{7a}$$

$$\bar{\sigma}' = \left[N_{x'}, \ N_{y'}, \ N_{x'y'}, \ M_{x'}, \ M_{y'}, \ M_{x'y'}, \ Q_{x'}, \ Q_{y'} \right]^{\mathrm{T}}, \tag{7b}$$

and the rigidity matrix D is given in Ref. [14],

$$D = \sum_{L=1}^{NL} \begin{bmatrix} D_m & D_c & 0 \\ D_c & D_b & 0 \\ 0 & 0 & D_s \end{bmatrix}, \tag{7c}$$

in which $D_m = Q_{ij} H_1$, $D_c = Q_{ij} H_2$, $D_b = Q_{ij} H_3$ and $D_s = Q_{ml} H_1$ are the membrane rigidity, coupling between inplane and bending rigidity, flexural rigidity and shear rigidity matrices respectively (where $i, j = 1, 2, 3$ and $m, l = 5, 4$). In the above relations, NL is the number of layers and

$$H_{n'} = \frac{1}{n'} \left(h_{L+1}^{n'} - h_L^{n'} \right), \quad n' = 1, 2, 3, 4, 5. \tag{7d}$$

As the strain–displacement matrix B and the rigidity matrix D are obtained in local coordinates, the same matrices should be used for the computation of the element stiffness matrix. Therefore the stiffness matrix is given by

$$K = \int_A B^T DB \; dA = \int_{-1}^1 \int_{-1}^1 B^T DB \, | J | \; d\xi \; d\eta. \tag{8}$$

The integration of the stiffness matrix is over the midsurface of the shell. Now, a temporal discretization of the dynamic equilibrium equations (1) is employed by approximating the accelerations and velocities using finite difference expressions [14–16]. In the present work, a central difference approximation is adopted, so that the accelerations and velocities can be written as

$$\ddot{a}^n = (a^{n+1} - 2a^n + a^{n-1})/\Delta t^2, \tag{9a}$$

$$\dot{a}^n = (a^{n+1} - a^{n-1})/(2\Delta t), \tag{9b}$$

where superscripts $n + 1$, n and $n - 1$ stand for three successive time intervals. The substitution of expressions given by (9a) and (9b) into equations (1) gives,

$$M(a^{n+1} - 2a^n + a^{n-1})/\Delta t^2 + f^n = q^n, \tag{10}$$

where, f^n is the internal resisting force vector and is given by

$$f^n = \int_A B^T \sigma^n \; dA = \int_{-1}^1 \int_{-1}^1 B^T \sigma^n \, | J | \; d\xi \; d\eta. \tag{11}$$

If the values of a^{n-1} and a^n etc., are known, the value of a^{n+1} can readily be found as,

$$a^{n+1} = M^{-1}\{\Delta t^2[-f^n + q^n] - Ma^{n-1} + 2Ma^n\}. \tag{12}$$

Since no stiffness and mass matrices of the complete element assemblage need to be calculated, the solution can essentially be carried out on the element level and relatively little high-speed storage is required. The method becomes even more effective if element stiffness and mass matrices of subsequent elements are the same, because in that case it is only necessary to calculate or read from back-up storage the matrices corresponding to the first element in the series. Using the central difference scheme, systems of very large order have been solved effectively.

It must be recognized that the effectiveness of the procedure depends on the use of a diagonal mass matrix and the neglect of general velocity-dependent damping forces. If only a diagonal damping matrix is included, the benefits of performing the solution on the element level are preserved. If the mass matrix M is diagonal, the computation at each time step is trivial. Unfortunately, for the quadrilateral isoparametric elements used in the spatial discretization, M is not diagonal, therefore a special mass matrix diagonalization scheme is used here, which is derived from a consistent mass matrix and is discussed elsewhere [14,17]. The mass matrix M in eqn. (1) is given by

$$M = \sum_{e=1}^{NE} M^e = \sum_{e=1}^{NE} \int_{\text{Area}} N^T mN \; dA, \tag{13a}$$

where

$$m = \begin{bmatrix} I_1 & & & & \\ & I_1 & & & \\ & & I_1 & & \\ & & & I_2 & \\ & & & & I_2 \end{bmatrix}, \quad (I_1, I_2) = \sum_{L=1}^{NL} \int_{h_L}^{h_{L+1}}(1, z'^2) \, \rho^L \; dz, \tag{13b}$$

in which I_1 and I_2 are normal inertia and rotary inertia respectively, and ρ^L is the material density of the Lth layer.

Numerical results and discussion

In the present study, the eight-node Serendipity and the nine-node Lagrangian quadrilateral superparametric shell elements were employed. It is well known that the shear correction coefficients depend on the lamination scheme and the lamina material properties. But due to lack of well accepted coefficients for finite shells, the transverse shear energy term in FOST is corrected using a multiplier 5/6 for all the materials except for the core of a sandwich shell where a coefficient of unity has been used. To evaluate the element stiffness properties based on the Gauss-quadrature (GQ) rule, the numerical selective reduced integration (SI) scheme viz., 3 × 3 for membrane, coupling between inplane and bending, and flexure terms, 2 × 2 for shear terms, and the reduced integration (RI) scheme, i.e., 2 × 2, for all terms in the energy expression, were employed. To obtain the load vector, 2 × 2 and 3 × 3 GQ rules were used respectively, while using RI and SI schemes. The external load is being applied on the shell mid-surface. The element mass matrix is evaluated using a 3 × 3 GQ rule in all the examples.

In transient analysis, the zero initial conditions on displacements and their derivatives were assumed for all cases. A quarter of the the shell is discretized for isotropic and cross-ply (0°/90°/0°/90°/ ...) laminates and a full shell discrete model is invariably used in angle-ply and other cases. An important note on symmetry line boundary conditions in fibre-reinforced laminated orthotropic/anisotropic composites can be found in Ref. [18]. The values of the principle radii of curvature of the middle surface are denoted by R_1 and R_2 ($R_1 = R_2 = R$ for spherical shells). The critical time step size depends on the mesh size, length/thickness ratio, degree of orthotropy, Poisson's ratio and the material density. In the present study, an estimate of the critical time step size, given by Tsui and Tong [19] for isotropic structures, is used with minor modification:

$$\Delta t \leqslant \Delta x \left\{ \frac{\rho(1 - \nu^2)/E_1}{2 + (\pi^2/12)(1 - \nu)\left[1 + 1.5(\Delta x/h)^2\right]} \right\}^{1/2}, \tag{14}$$

where Δx is the smallest distance between adjacent nodes in any quadrilateral element used.

Example 1

A spherical cap clamped on the boundary, shown in Fig. 2, is subjected to a distributed step pressure of 600 lb/in². The dimensions and properties of the shell are as follows: internal radius $R_1 = 22.27$ in ($R = 22.475$ in); thickness of shell, $h = 0.41$ in; semi-angle = 26.67°; elastic modulus, $E = 10.5 \times 10^6$ lb/in²; mass density $\rho = 2.45 \times 10^{-4}$ lb s²/in⁴, Poisson's ratio = 0.3, time step $t = 1$ ms. Figure 2 shows the centre vertical displacement of the spherical cap for the analysis based on both the present seven 8-noded quadrilateral elements and ten 8-noded axisymmetric elements [15]. Since the geometry of the shell is thin (large ratio of a/h), the difference between the present element with FOST and an axisymmetric element [15] is almost negligible, except in the regions of local minimum and maximum.

Example 2

A quarter of a composite-sandwich spherical shell was analysed with a 2 × 2 mesh subjected to a uniformly distributed static loading $q = 1$ N/cm². A frontal technique is used
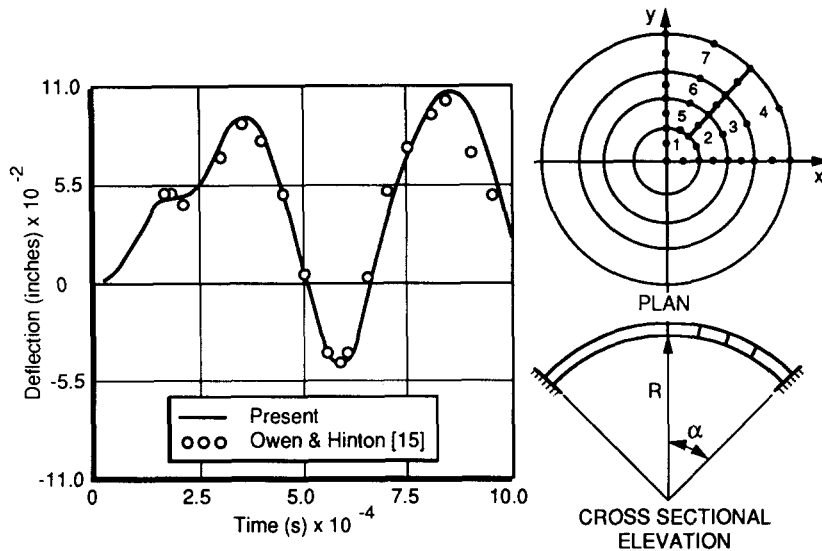
Fig. 2. Transient response of a clamped spherical cap.

to solve the static equilibrium equations. The stacking sequence of a layered shell is $(0°/90°/0°/90°/core/90°/0°/90°/0°)$ and the thickness of each stiff layer is $0.05h$ and that of the core is $0.6h$. Keeping the arc lengths $a = b = 32$ cm constant, the radius of the middle surface, R, and thickness, h, were varied. The following material properties were used: for face sheets (graphite/epoxy prepreg system), $E_1 = 1.308 \times 10^7$ N/cm^2, $E_2 = 1.06 \times 10^6$ N/cm^2, $G_{12} = G_{13} = 6.0 \times 10^5$ N/cm^2, $G_{23} = 3.9 \times 10^5$ N/cm^2, $\nu_{12} = 0.28$, $\rho = 15.8 \times 10^{-6}$ N s^2/cm^4; and for the core (U.S. commercial aluminium honeycomb), $G_{23} = 1.772 \times 10^4$ N/cm^2, $G_{13} = 5.206 \times 10^4$ N/cm^2, $\rho = 0.1009 \times 10^{-5}$ N s^2/cm^4.

Table 1 shows the centre transverse deflection for the 8-node and 9-node quadrilateral shell elements with different boundary conditions: simply supported and clamped. The results are presented for RI and SI schemes and also varying a/h ratios from 10 to 1000 and R/a ratios from 1 to infinity. From this table, it is observed that for a thick shell, $a/h = 10$, the difference in the results between 8-node and 9-node elements is almost negligible. For a thin shell, $a/h = 100$, as R/a increases from unity to infinity there is not much appreciable difference in the simply supported case, but in the clamped shell the percentage difference with respect to the 9-node element is about -1.5, -4, and -7 for $R/a = 1$, 5 and 10 respectively, and for $R/a = 50$, 100 and ∞, it is about -11. For $a/h = 500$, the percentage difference between 8-node and 9-node elements, with respect to the latter, varies from about 2% to -5% for $R/a = 1$ to ∞ for the case of simply supported shells, whereas in the clamped boundary conditions for $R/a = 1$ and 5 it is about 3% and -3% respectively, and for $R/a = 10$ it is -7%, but it is -46%, -56% and -60% for $R/a = 50$, 100 and ∞ respectively. In the case of very thin shells, $a/h = 1000$, the percentage difference varies from about 4.8% to -3.75% for $R/a = 1$ to 50, and 11.5% and 20% for $R/a = 100$ and ∞ respectively, in simply supported shells, but in clamped shells it varies from about 3.5% to -70% for $R/a = 1$ to ∞. This significant difference in the results of 8-node and 9-node elements is noted in the case of very thin shells $(a/h = 500$ and 1000) with $R/a = 50$, 100 and ∞ (plate).

Since there are no analytical results available for thin and very thin sandwich-type fibre-reinforced composite spherical shells, the present results are not validated, but it is observed that as such there is no appreciable difference between RI and SI schemes even for

Table 1
Center deflection ($w \times$ Factor) in cm of composite-sandwich spherical shells for static load.

a/h	Factor	R/a	Simply supported				Clamped			
			8-node		9-node		8-node		9-node	
			SI	RI	SI	RI	SI	RI	SI	RI
10	0.0001	1	2.4023	2.4102	2.4056	2.4147	0.7036	0.7000	0.7059	0.7031
		5	5.6202	5.6230	5.6345	5.6374	2.1551	2.1555	2.1665	2.1669
		10	5.8347	5.8368	5.8499	5.8521	2.2991	2.2997	2.3114	2.3118
		50	5.9066	5.9085	5.9221	5.9240	2.3493	2.3498	2.3618	2.3622
		100	5.9089	5.9107	5.9244	5.9263	2.3509	2.3514	2.3634	2.3638
		∞	5.9096	5.9115	5.9252	5.9270	2.3514	2.3520	2.3639	2.3643
100	0.001	1	4.5369	4.5900	4.5390	4.5902	0.7302	0.7320	0.7392	0.7451
		5	109.62	110.49	109.93	110.78	21.639	21.837	22.567	22.814
		10	260.04	261.43	261.05	262.43	53.323	53.635	57.484	57.881
		50	450.95	451.31	453.18	453.55	94.054	94.229	105.79	106.04
		100	461.45	461.70	463.76	464.02	96.317	96.476	108.59	108.82
		∞	465.03	465.24	467.36	467.59	97.082	97.235	109.55	109.77
500	0.01	1	2.4068	2.6392	2.3547	2.5037	0.4213	0.5417	0.4097	0.5233
		5	60.875	61.239	61.060	61.432	8.0731	8.0919	8.2874	8.4190
		10	254.99	256.66	251.56	251.53	39.130	39.220	41.963	42.525
		50	3165.6	3182.3	3263.3	3280.8	387.82	388.34	715.31	720.44
		100	4645.3	4654.5	4881.4	4892.6	493.42	493.88	1111.4	1115.8
		∞	5485.7	5488.2	5826.9	5829.7	541.14	541.56	1353.6	1356.6
1000	0.1	1	0.4914	0.4950	0.4801	0.4722	0.0869	0.1177	0.0839	0.1124
		5	12.191	12.396	12.324	12.867	1.5478	1.5916	1.6880	1.9156
		10	48.795	49.105	48.907	49.196	6.4188	6.4282	6.6075	6.7129
		50	1060.9	1069.8	1102.3	1111.2	141.08	141.18	225.88	228.49
		100	2311.8	2321.3	2617.7	2631.6	246.24	246.43	574.06	578.18
		∞	3733.4	3734.8	4661.1	4663.4	321.58	321.84	1082.5	1084.9

SI—Selective Integration, RI—Reduced Integration.

very thin shells ($a/h = 1000$). It is concluded that the maximum error (up to 70%) between 8-node and 9-node elements particularly for very thin ($a/h = 1000$) composite-sandwich spherical shells with clamped boundary conditions could be due to either locking phenomenon or spurious mechanisms i.e., zero-energy modes, by either of these elements.

Example 3

A simply supported, five layer ($0°/90°/\text{core}/0°/90°$) unsymmetric composite-sandwich spherical shell under suddenly applied uniformly distributed pulse loading ($q = 1 \text{ N/cm}^2$) with a 3×3 mesh quarter model is analyzed for two cases: considering and neglecting G_{23} and G_{13} of the stiff layers. The same material properties which were given in Example 2 with the RI scheme are used here. The thickness of each stiff layer is 0.1 h and that of the core is 0.6 h. The principle radius of curvature of the middle surface R is 96 cm and arc lengths $a = b = 32$ cm. The variation of the centre transverse deflection for length/thickness ratio (a/h) equal to 10 and 100 is presented in Fig. 3. From these plots it is observed that the simplified sandwich theories, which account for only bending rigidities of the facings and shear rigidities of the core material, predict lower values of frequencies and overestimate deflections. Considerable deviation in the results is noted if the shear rigidities for the facings are also taken into account, in addition to the bending rigidities. But, in thin shells this effect is almost negligible.
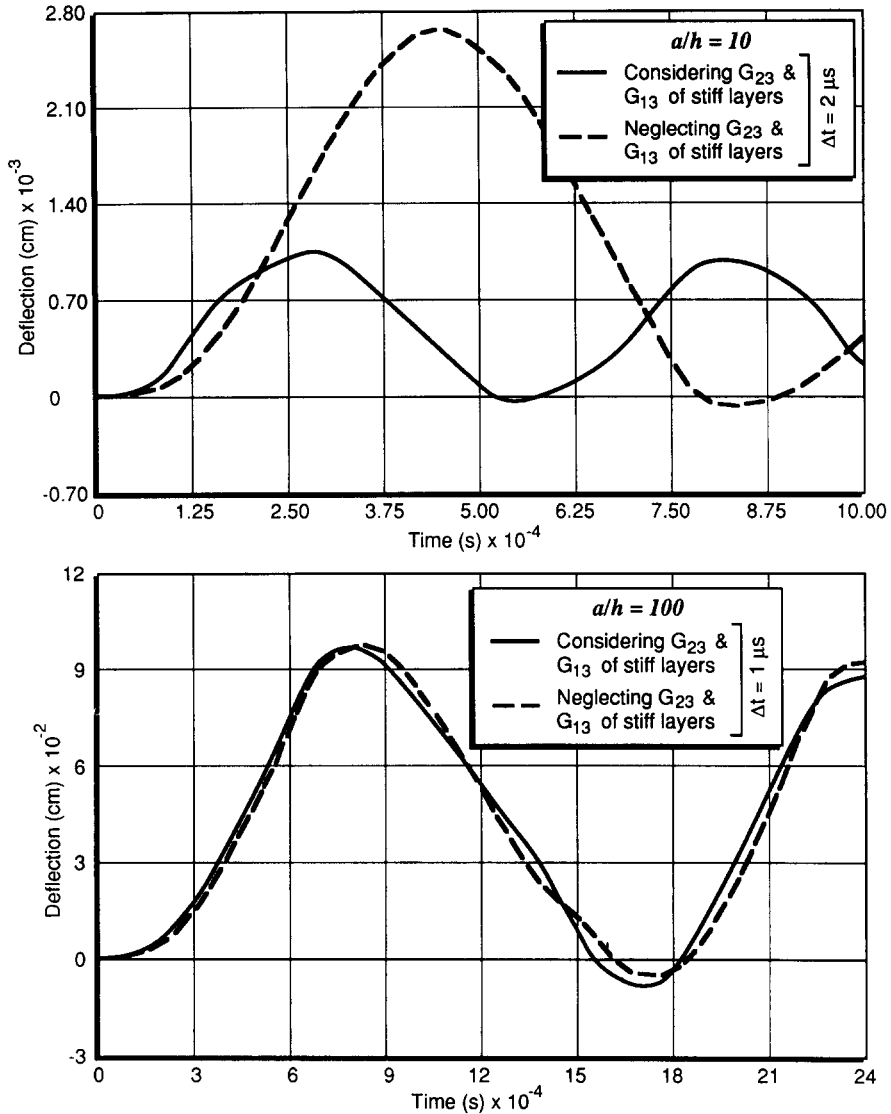
Fig. 3. Effect of transverse shear modulus of stiff layers ($R/a = 3$, quarter spherical shell with 3×3 mesh, stacking sequence $= 0°/90°/\text{core}/0°/90°$, thickness $= 0.1\ h /0.1\ h /0.6\ h /0.1\ h /0.1\ h$).

Example 4

To further investigate the effect of material orthotropy on the centre transverse deflection, an entire composite spherical shell is analyzed with a 4×4 mesh and clamped boundary conditions on all the four sides. The problem under consideration is a six-layer symmetric angle-ply ($0°/45°/-45°/-45°/45°/0°$) laminate, which is used in F-16 Aircraft by General Dynamics Corporation, Ft. Worth. Individual layers are assumed to be orthotropic with the following properties: E_1/E_2 is varied (i.e. 10, 25 and 40), $G_{23} = 0.2\ E_2$, $G_{12} = G_{13} = 0.5\ E_2$, $\nu_{12} = 0.25$. The material density, ρ, Young's modulus in transverse direction, E_2, and uniformly distributed step load are taken equal to unity. The RI scheme is used to evaluate the stiffness properties. The non-dimensionalized centre deflections with time for $R/a = 2$
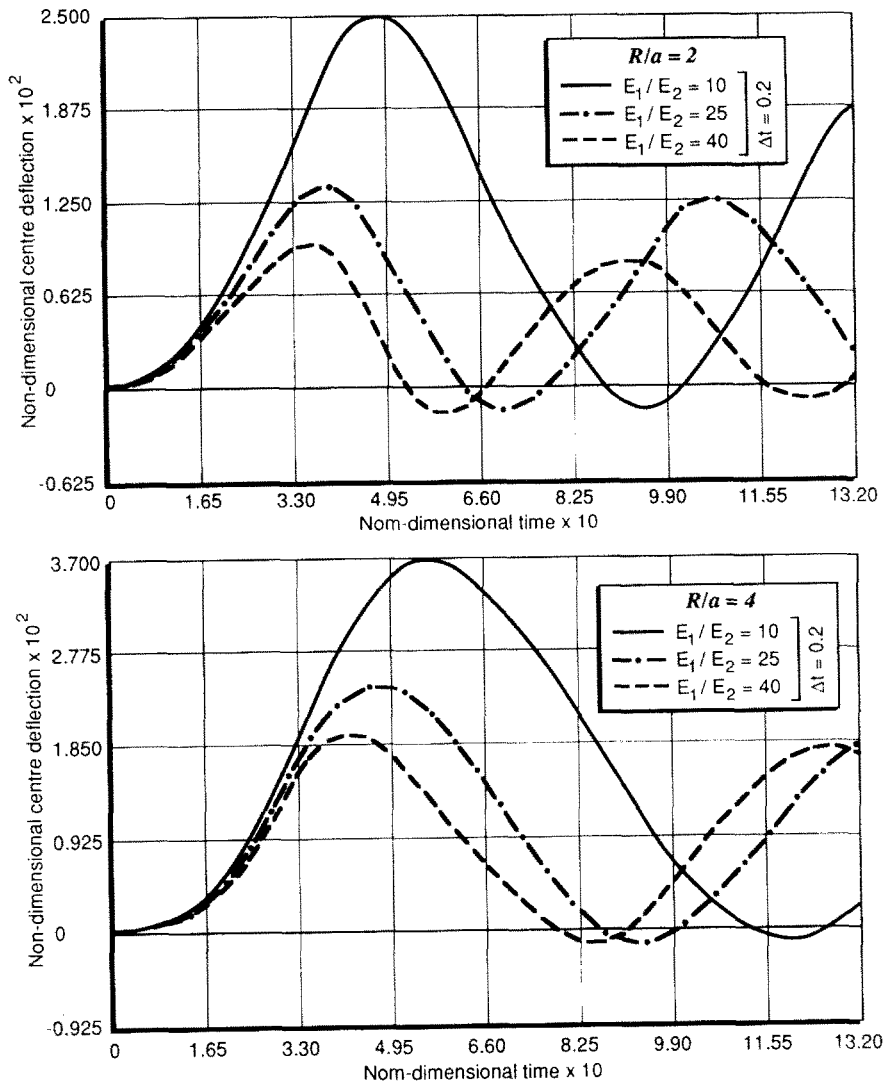
Fig. 4. Effect of degree of orthotropy on the transient response of a clamped spherical shell ($a/h = 10$, full shell with 4×4 mesh, stacking sequence $= 0°/45°/-45°/-45°/45°/0°$).

and 4 (arc length $a = 32$ cm and thickness $h = 3.2$ cm) are shown in Fig. 4. It is found that as the material orthotropy increases the deflection decreases, thus frequency increases.

Conclusions

The behavior of eight- and none-node quadrilateral superparametric shell elements for thick, thin and very thin fiber-reinforced laminated composite-sandwich spherical shells is studied. Numerical results from the static and transient analysis of sandwich shells based on the first-order shear deformation theory are presented. The significance of the effect of transverse shear moduli of stiff layers and the degree of orthotropy on the sandwich and composite shells for different ratios of a/h and R/a is highlighted. The centre deflections

vary more rapidly with greater ratios of R/a, for deep shells (i.e. for large ratios of a/h) than for shallow shells (i.e. for small ratios of a/h). All the results presented here for sandwich shells must be validated by an independent investigation.

Acknowledgement

References

[1] F.J. PLANTEMA, *Sandwich Construction*, Wiley, New York, 1966.

[2] H.C. ALLEN, *Analysis and Design of Structural Sandwich Panels*, Pergamon, London, 1969.

[3] L.M. HABIP, "A review of recent work on multilayered structures", *Int. J. Mech. Sci.* 7, pp. 389–393, 1965.

[4] L.M. HABIP, "A survey of modern developments in analysis of sandwich structures", *Appl. Mech. Rev.* 18, pp. 93–98, 1965.

[5] E. REISSNER, "The effect of transverse shear deformation on the bending of elastic plates", *J. Appl. Mech. ASME* 12, pp. A69–A77, 1945.

[6] E. REISSNER, "Finite deflections of sandwich plates", *J. Aerosp. Sci.* 15, pp. 435–440, 1948; 17, p. 125, 1950.

[7] G.R. MONFORTON and L.A. SCHMIT, "Finite element analysis of sandwich plates and cylindral shells with laminated faces", *Proc. 2nd Conf. on Matrix Methods in Structural Mechanics*, Wright–Patterson Air Force Base, Ohio, pp. 573–616, 1969.

[8] K.M. AHMED, "Static and dynamic analysis of sandwich structures by the method of finite elements", *J. Sound Vib.* 18, pp. 75–91, 1971.

[9] T.J.R. HUGHES and W.K. LIU, "Nonlinear finite element analysis of shells: Part I. Three-dimensional shells", *Comput. Methods Appl. Mech. Eng.* 27, pp. 331–362, 1981.

[10] S. AHMAD, B.M. IRONS and O.C. ZIENKIEWICZ, "Analysis of thick and thin shell structures by curved elements", *Int. J. Numer. Methods Eng.* 2, pp. 419–451, 1970.

[11] T. BELYTSCHKO, H. STOLARSKI, W.K. LIU, N. CARPENTER and J.S.J. ONG, "Stress projection for membrane and shear locking in shell finite elements", *Comput. Methods Appl. Mech. Eng.* 51, pp. 221–258, 1985.

[12] R.V. MILFORD and W.C. SCHNOBRICH, "Degenerated isoparametric finite elements using explicit integration", *Int. J. Numer. Methods Eng.* 23, pp. 133–154, 1986.

[13] T. KANT and D. DATYE, "Finite elements available for the analysis of curved thin walled structures", in: *Finite Element Applications to Thin-Walled Structures*, edited by Ed. J.W. BULL, Elsevier Applied Science, London, 1990.

[14] T. KANT and MALLIKARJUNA, "Transient dynamics of composite sandwich plates using 4-, 8-, 9-noded isoparametric quadrilateral elements", *Finite Elements in Analysis and Design* 5, pp. 307–318, 1989.

[15] D.R.J. OWEN and E. HINTON, *Finite Elements in Plasticity — Theory and Practice*, Pineridge Press, Swansea, UK, 1980.

[16] K.J. BATHE, *Finite Element Procedures in Engineering Analysis*, Prentice-Hall, Englewood Cliffs, NJ, 1982.

[17] E. HINTON, T. ROCK and O.C. ZIENKIEWICZ, "A note on mass lumping and related processes in the finite element method", *Earthquake Eng. Struct. Dyn.* 4, pp. 245–249, 1976.

[18] MALLIKARJUNA. "An important note on symmetry line boundary conditions in fibre-reinforced laminated anisotropic composites", *Comput. Struct.* 38, pp. 669–671, 1991.

[19] T.Y. TSUI and P. TONG, "Stability of transient solution of moderately thick plates by finite difference methods", *AIAA J.* 9, pp. 2062–2063, 1971.